J Biomol NMR (2011) 50:403–410
DOI 10.1007/s10858-011-9526-0

ARTICLE

A segmental labeling strategy for unambiguous determination of domain–domain interactions of large multi-domain proteins

Jianglei Chen · Jianjun Wang

Received: 5 May 2011 / Accepted: 16 June 2011 / Published online: 6 July 2011

Abstract NMR structural determination of large multi-domain proteins is a challenging task due to significant spectral overlap with a particular difficulty in unambiguous identification of domain–domain interactions. Segmental labeling is a NMR strategy that allows for isotopically labeling one domain and leaves the other domain unlabeled. This significantly simplifies spectral overlaps and allows for quick identification of domain–domain interaction. Here, a novel segmental labeling strategy is presented for detection of inter-domain NOEs. To identify domain–domain interactions in human apolipoprotein E (apoE), a multi-domain, 299-residues α-helical protein, on-column expressed protein ligation was utilized to generate a segmental-labeled apoE samples in which the N-terminal (NT-) domain was ^{2}H(99%)/^{15}N-labeled whereas the C-terminal (CT-) domain was either ^{15}N- or ^{15}N/^{13}C-labeled. 3-D ^{15}N-edited NOESY spectra of these segmental-labeled apoE samples allow for direct observation of the inter-domain NOEs between the backbone amide protons of the NT-domain and the aliphatic protons of the CT-domain. This straightforward approach permits unambiguous identification of 78 inter-domain NOEs, enabling accurate definition of the relative positions of both the NT- and the CT-domains and determination of the NMR structure of apoE.

Keywords NMR · Segmental labeling · NOESY · NOE · Inter-domain interaction · apoE3

J. Chen · J. Wang (✉)
Department of Biochemistry and Molecular Biology,
School of Medicine, Wayne State University,
Detroit, MI 48201, USA
e-mail: jjwang@med.wayne.edu

Introduction

Solution NMR spectroscopy is a powerful structural biology technique to determine protein structures, dynamics and site-specific molecular interactions. The NMR size limitation of proteins has been dramatically reduced by TROSY (Pervushin et al. 1997), deuteration (Gardner and Kay 1998) as well as the hardware development, such as higher magnetic fields and cryogenically cooled probe. Other NMR techniques, such as methyl labeling (Tugarinov and Kay 2005; Philipps et al. 2003), site-directed spin-labeling (Ignatova and Gierasch 2004) and residue dipolar coupling (Bax 2003) are developed to obtain additional distance and orientation restraints for protein structure refinement, especially for large proteins. Special labeling strategies to generate isolating labeled NMR samples have also been developed and used to study interactions between proteins, peptides and ligands (Golovanov et al. 2007; Masterson et al. 2008; Ferrage et al. 2010). Segmental isotope-labeling technology combines the independent labeling scheme and native chemical ligation, providing a useful approach to significantly reduce spectral overlaps and to quickly identify domain–domain interactions of large multi-domain proteins (Zhao et al. 2008; Vitali et al. 2006; Zhang et al. 2007).

Human apoE is a 299-residue lipid transport protein that is critical to several major human diseases including heart disease and Alzheimer's disease (Weisgraber 1994; Huang et al. 2004; Hatters et al. 2006). Recently, it has also been reported that apoE is associated with the development of obesity (Karagiannides et al. 2008), type 2 diabetes (Ma et al. 2008) and infectious diseases (Burt et al. 2008; Mahley et al. 2009). ApoE is a multi-domain protein that contains a 22 kDa NT-domain (residue 1–168) and a 10 kDa CT-domain (residue 216–299), linked by a protease-

sensitive hinge domain. Three common apoE isoforms differ at one amino acid: apoE3 has C112/R158, apoE4 has R112/R158 and apoE2 has C112/C158 (Weisgraber et al. 1981). ApoE manifests critical isoform-specific effects on several major human diseases (Huang 2010), and this isoform-specific effect is attributed to the difference of domain–domain interactions (Hatters et al. 2006).

Since the domain–domain interaction of apoE is hypothesized to regulate its biological functions, an accurate identification of domain–domain interaction is critical for us to understand the structural basis of apoE's functions. The crystal structures of the NT-domain of apoE isoforms indicate subtle variations (Wilson et al. 1994; Dong et al. 1996). The inter-change of C112R in apoE4-NT leads to a new salt bridge between E109 and R112, causing the side chain of R61 to adopt an exposed position (Dong et al. 1994). Mutagenesis study suggested that the R61 sidechain might form a salt bridge with E255, whereas apoE3 and apoE2 were hypothesized to lack this salt bridge (Dong and Weisgraber 1996). It is further suggested that this single salt-bridge in apoE4 is critical to apoE's isoform-specific effects on human diseases (Hatters et al. 2006). However, this putative domain-interaction remains a hypothesis due to lack of high-resolution structures of full-length apoE.

ApoE forms a mixture of different oligomers, hindering structural determination of this important protein (Weisgraber 1994; Zhang et al. 2007; Mahley et al. 2009). Using protein-engineering techniques, we strategically mutated five residues in the CT domain apoE, allowing us to prepare a biologically active monomeric apoE CT domain (Fan et al. 2004). We also generated a biologically active full-length monomeric apoE3 using the same mutations, which retained the properties of the parent protein and allowed for collection of the high-quality NMR data (Zhang et al. 2007). To further simplify NMR spectra, several segemental-labeled monomeric apoE3 NMR samples were prepared (Zhao et al. 2008), allowing for a complete backbone assignment (Zhang et al. 2008). However, during NOESY assignment, unambiguously assigning inter-domain NOEs was a major difficulty due to severe spectral overlaps of this 299-residue α-helical protein, even with 4-D ^{15}N/^{13}C-edited NOESY experiments.

To solve this problem, special segmental-labeled apoE samples were prepared, in which the NT-domain was ^{2}H(99%)/^{15}N-labeled, whereas the CT-domain was only ^{15}N-labeled or ^{13}C/^{15}N-labeled. Deuteration of the NT-domain completely depleted aliphatic protons of the residues within this domain, allowing for observation of three patterns of NOE crosspeak using 3-D ^{15}N-edited NOESY (Fig. 1): (1) the intra- and inter-domain NOEs between the amide protons of the residues in the NT- and/or CT-domain (1a, Fig. 1), the inter-domain NOEs from the NT-domain amide protons to the aliphatic protons in the CT-domain

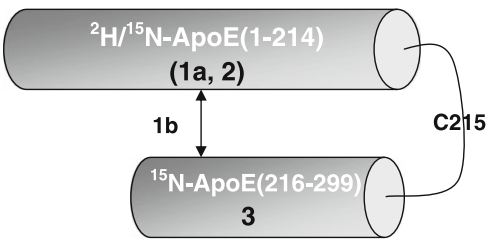

Crosspeaks in a 3D ^{15}N-edited NOESY Spectrum of the special segmental-labeled apoE sample

1. NOE crosspeaks of residue X in the NT-domain.
   a. Intra- and inter-domain NOE crosspeaks of amide-amide protons of residue X in the NT-domain and other residues in the NT- and/or CT-domain.
   b. Inter-domain NOE crosspeaks from the backbone amide proton of residue X in the NT-domain to the aliphatic protons of the residues *only* in the CT-domain.
2. NOE crosspeaks of residue Y in the NT-domain: NOEs from the amide proton of residue Y to the other amide protons (NT and/or CT).
3. NOE crosspeaks of residue Z in the CT-domain: NOEs from the amide proton of residue Z to the other amide protons (NT and/or CT) and the aliphatic protons *only* in the CT-domain.

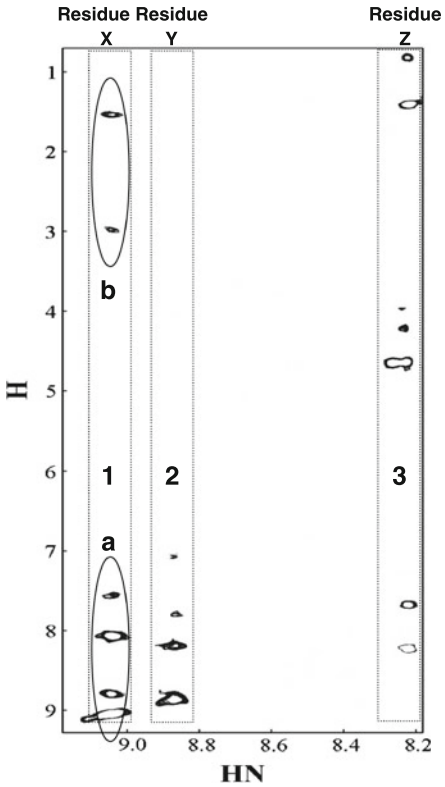

Fig. 1 Schematic diagram of 3-D ^{15}N-edited NOESY NMR spectroscopy to determine inter-domain long range NOEs using special segmental-labeled apoE protein. Three different cases of NOE cross-section are *boxed* and correspondingly indicated and interpreted

(1b, Fig. 1); (2) the amide proton NOEs from the residues of the NT-domain to the residues in the NT-domain and/or the CT-domain (2, Fig. 1); (3) the NOEs from amide protons of the residues in the CT-domain to the amide protons of the residues in both NT and CT-domains and to the aliphatic protons of the residues in the CT-domain only (3, Fig. 1). This special segmental-labeled apoE displayed not only the intra-domain amide–amide NOEs within the NT- and CT-domains and the inter-domain amide–amide NOEs between CT and NT-domains (1a and 3, Fig. 1), but also the inter-domain amide/aliphatic NOEs from the amide proton (exchangeable) of the NT-domain to the aliphatic protons in the CT-domain (1b, Fig. 1). Since the CT-domain only contained 85-residues, the spectral was significantly simplified, allowing for unambiguous identification of the inter-domain long range NOEs for structural determination of this large α-helical multi-domain apoE protein.

Materials and methods

Preparation of special segmental-labeled apoE samples

Following the established on-column native chemical ligation protocol, two special segmental-labeled monomeric apoE samples were prepared (Zhao et al. 2008). Briefly, either ^{15}N-labeled or ^{13}C/^{15}N-labeled apoE-CT, apoE(C215–299) were expressed and purified using pET30(+) bacterial vector, which contained a long his-tag. After removal of the his-tag by factor Xa, the apoE (C215–299) was generated, containing a free cysteine at the N-terminus that was ready for ligation. The ^{15}N-labeled apoE(1–214) was then prepared in 99.9% D_2O using the optimized apoE(1–214)/pTWIN bacterial expressions (Cui et al. 2006). During the purification of 300 ml bacterial expressed ^{2}H(99%)/^{15}N-labeled apoE(1–214), the chitin bead column (6 ml) was washed with 500 ml binding buffer in a cold room and then transferred from the column into a small bottle and the supernatant was carefully removed. The ligation-ready apoE(C215–299) (20 mg) was dissolved into 1 ml (20 mg/ml) ligation buffer and mixed well with the chitin beads that bind to ^{2}H(99%)/^{15}N-labeled apoE(1–214). The ligation reaction was initiated by the addition of 240 μl of thiol phenol. The ligation reaction was maintained in room temperature for 20–24 h with a gentle stir. An aliquot of chitin bead mixture was taken out and mixed with 4 × SDS loading buffer for a SDS–PAGE to ensure that the ligation reaction was complete.

The ligation mixture was gently spun down and the chitin beads were washed with 5 × volume of loading buffer. All supernatants were combined and mixed with 500 μl of new chitin beads to remove any intein-CBD in the supernatant. The supernatant was diluted to 100 ml with loading buffer and then loaded on a Heparin Sepharose^{TM} CL-6B column. The CL-6B column was washed with 100 ml loading buffer and then eluted with elution buffer containing 200 mM NaCl. The elution was dialyzed against water containing 20 mM ammonium bicarbonate and then lyophilized. Using this method, we prepared two segmental-labeled monomeric apoE3 for this study.

NMR sample conditions

NMR samples comprising of 1.0 mM monomeric apoE3 protein were prepared in 10% D_2O, 100 mM potassium phosphate pH 6.8, 10 mM EDTA, 0.05 mM NaN_3, 500 mM urea and 10 mM DTT-d_{10}. The proton chemical shift was referenced using DSS (2,2-dimethyl-2-silapentane-5-sulfonate) at 0.0 ppm.

NMR experiments and inter-domain NOE assignment

3-D ^{15}N-edited NOESY NMR spectra were acquired at 30°C on a 600 MHz Varian INOVA spectrometer equipped with a cryogenic probe. NMR data were processed on a SGI workstation using nmrPipe (Delaglio et al. 1995) and the assignment was achieved using the PIPP (Garrett et al. 1991) and nmrview (Johnson and Blevins 1994). ApoE structures were calculated using software package CYANA (Guntert 2004) based on distance constraints derived from 3-D/4-D Nuclear Overhauser Effect Spectroscopy (NOESY) experiments including ^{15}N-edited NOESY and 4-D-^{13}C^{15}N-edited NOESY using 50% deuterated uniformly triple labeled apoE samples, plus 78 unambiguous inter-domain NOEs obtained with these special segmental-labeled apoE samples. The addition of these 78 inter-domain distance constraints allowed for defining of the specific and accurate position of the two domains of apoE. The structure cartoons were displayed using Pymol (DeLano Scientific, Palo Alto).

Results and discussion

For large multi-domain α-helical proteins like apoE, it is necessary to use triple-labeled protein sample with ^{2}H/^{13}C/^{15}N for enhancement of the signal-to-noise. This causes a problem with NOESY spectra since no protons are available in the triple-labeled apoE. Segmental-labeled apoE samples with one triple-labeled domain and another double-labeled domain with ^{13}C/^{15}N allow for collection of the NOESY spectra of the double-labeled domain. However, these segmental-labeled apoE samples only display inter-domain NOEs of backbone amide protons that show small chemical shift dispersion for α-helical proteins. In

addition, residues in the helical region also display many $d_{NN}(i, i \pm 1)$ and $d_{NN}(i, i \pm 2)$ NOEs in the narrow backbone amide proton region, causing major spectral overlaps of this large α-helical protein. This results in significant ambiguity for the assignment of inter-domain NOEs.

To unambiguously identify inter-domain NOEs, two special segmental-labeled apoE samples were prepared in which the NT-domain was ^{2}H (99%)/^{15}N-labeled and the CT-domain was either ^{15}N- or $^{15}N/^{13}C$-labeled. Here we used the monomeric apoE3 mutant to prepare these special segmental-labeled apoE3 samples. Previously, we demonstrated that the introduction of these mutations in the apoE CT-domain did not change the properties of full-length apoE3, and the monomeric apoE3 maintained the structure, stability and biological functions of wild-type apoE3 (Zhang et al. 2007). Most importantly, this monomeric apoE3 also displayed similar domain–domain interactions between the NT- and CT-domains (Zhang et al. 2007). These special segmental-labeled samples significantly improved spectral quality and allowed for direct detection and assignment of inter-domain NOEs. First, the perdeuteration of the NT-domain significantly reduced the proton density and enhanced the signal-to-noise of the NOESY spectra as compared to those of the partially deuterated and uniformly triple-labeled protein samples (Fig. 2a). Second, the NOESY spectra were greatly simplified in the sidechain areas (Fig. 2b) since the aliphatic protons of the NT-domain were replaced by deuterium. In this case, the sidechain NOEs were either from intra-domain NOEs of CT-domain (85 residues) or from inter-domain NOEs between the amide protons of the NT-domain and aliphatic protons of the CT-domain. This allowed us to observe three type of NOEs as summarized in Fig. 1, including unambiguous inter-domain NOEs (1b, Fig. 1).

An example is shown in Fig. 3a, displaying several inter-domain NOEs from γ-proton of E234 to amide proton of E132. Clearly, only one NOE was observed in the left panel using this special segmental-labeled sample, whereas more NOEs were found in the right panel using a 50% deuterated triple-labeled apoE, including both intra- and inter-domain NOEs. The spectral simplifications were further confirmed in Fig. 3b, c. The NOESY spectrum of the uniform labeled apoE sample endured severe overlaps for residues E13, A138 and L144 (Fig. 3b, right panels), displaying overlapping crosspeaks that were mainly short and medium range NOEs within the NT-domain. It is difficult to confidently assign long range NOEs in this spectrum. In contrast, the same spectral strip of the special segmental-labeled apoE only showed inter-domain NOEs (Fig. 3b), and the simplified spectrum was also observed for residue S139 (Fig. 3c), allowing us to confidently

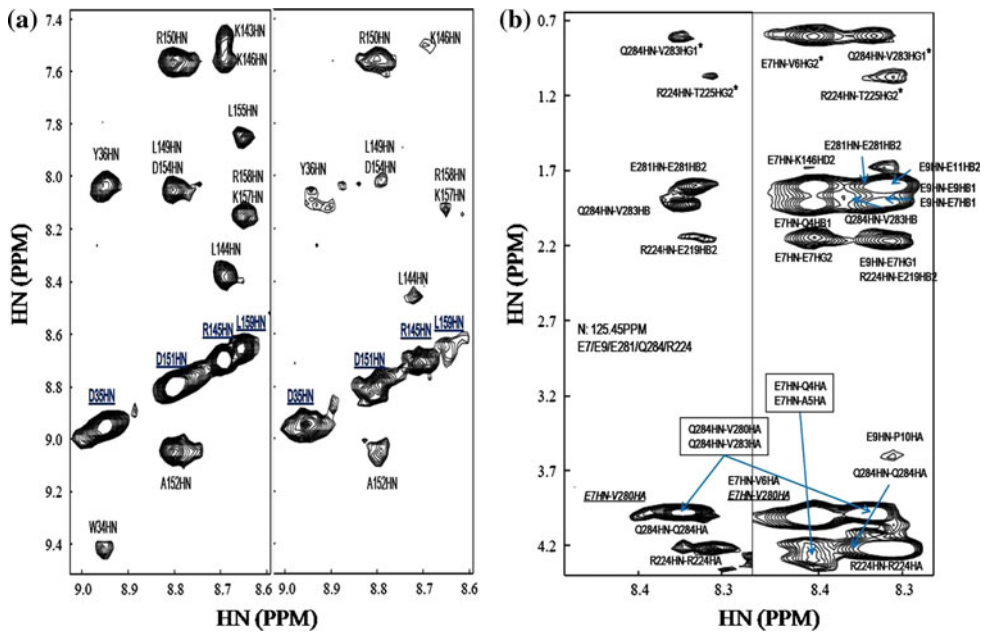

Fig. 2 Spectral comparison between this special segmental-labeled apoE and uniformly triple labeled apoE with 50% deuteration using the strips in 3-D ^{15}N-edited NOESY. **a** Significant enhanced signal–noise of the spectrum of the special segmental-labeled apoE (*left panel*) as compared to the same NOESY spectral strip of the uniformly triple-labeled (50% deuteration) apoE (*right panel*). The diagonal peaks are labeled in *blue* while other cross-peaks are labeled in *black*. **b** Significantly simplified spectra of this special segmental-labeled apoE (*left panel*) as compared with the same NOESY spectral strip of uniformly triple-labeled apoE (*right panel*). The NOE assignments are labeled, the inter-domain long range assignment E7HN-V280HA is *underlined*

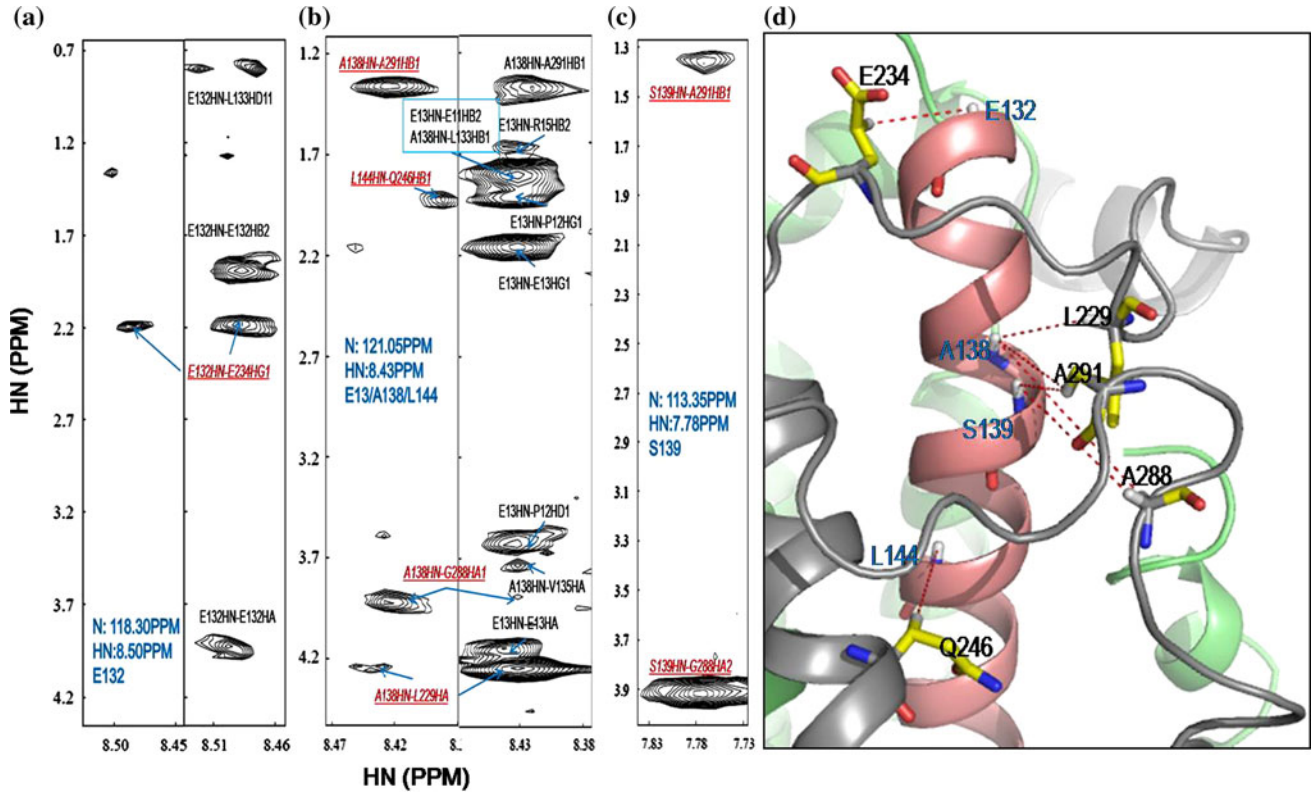

Fig. 3 Unambiguous NOE assignments on ^{15}N-edited NOESY and corresponding structure region using this special segmental-labeled apoE3. **a**, **b** Side-by-side comparison between segmental labeling (*left panel*) and uniform labeling (*right panel*) of selected aliphatic region of (**a**) E132 and (**b**) E13/A138/L144. **c** Several specific inter-domain NOEs–S139 amide proton can be assigned using segmental labeling NOESY spectra. In **a**, **b** and **c**, unambiguous inter-domain NOEs are labeled in *red* while others in *black*. **d** Corresponding structure region of the residues in **a**, **b** and **c**. The residues in the CT-domain contributing to the inter-domain NOEs are displayed in *yellow* sticks and labeled in *black*, while residues in the NT-domain only display *backbone sticks* and are labeled in *blue*. The assigned inter-domain NOEs are indicated by *red dotted lines*

assign these long-range NOEs. Indeed, the spectral regions of Fig. 3a–c provides seven unambiguous inter-domain NOEs for structural determination, permitting for accurate defining the loops (residues 224–235 and 277–299) in the CT-domain against the helix 4 of the NT-domain. These NOE distance restraints were confirmed in the final NMR structure of apoE and found that they displayed proper distances between the CT-domain (Grey) and the NT-domain (Pink) (Fig. 3d).

Figure 4 shows several inter-domain NOEs between Helix 3 in the NT-domain and a helix in the CT-domain. As demonstrated in Fig. 4a, the special segmental-labeled apoE only gives inter-domain NOEs, resulting in well-resolved crosspeaks for unambiguous assignments. In the overlapping region of the uniformly triple-labeled apoE sample, the spectrum of this special segmental-labeled apoE is significantly simplified. Figure 4b shows a zoom-in cross-section of residues A99, A100 and L261, which have very close chemical shift for their amide protons, providing reliable inter-domain NOE assignments. In this spectral region, inter-domain NOEs between amide protons of A99/A100 and sidechain protons of the residues in the CT-domain, such as 251, 256, 259 and 260, were unambiguously assigned. Using these NOEs as distance constraints, the long helix in the CT-domain (grey) and the long helix (Helix 3) of the NT-domain (pink) were confidently positioned in the final apoE structure (Fig. 4c).

Using an iterative assignment procedure, 78 unambiguous inter-domain NOEs were obtained that serve as the initial inter-domain distance restraints for structural calculation of apoE. In particular, no long-range NOEs were observed between residues R61 and E255 as well as between surrounding their residues, suggesting that it was unlikely for these two residues in apoE3 to form a salt-bridge. This is inconsistent with the literature, suggesting that apoE4 contains this salt-bridge that is hypothesized to be critical for its functions in Alzheimer's disease (Dong and Weisgraber 1996). However, there was no direct experimental evidence to exclusively support this salt-bridge. In fact, the inter-domain NOE pattern obtained from this study suggests that R61 is far apart from E255.

These unambiguous inter-domain NOEs permitted the generation of the initial apoE structure that was then used to guide further inter-domain NOE assignment in the 3-D

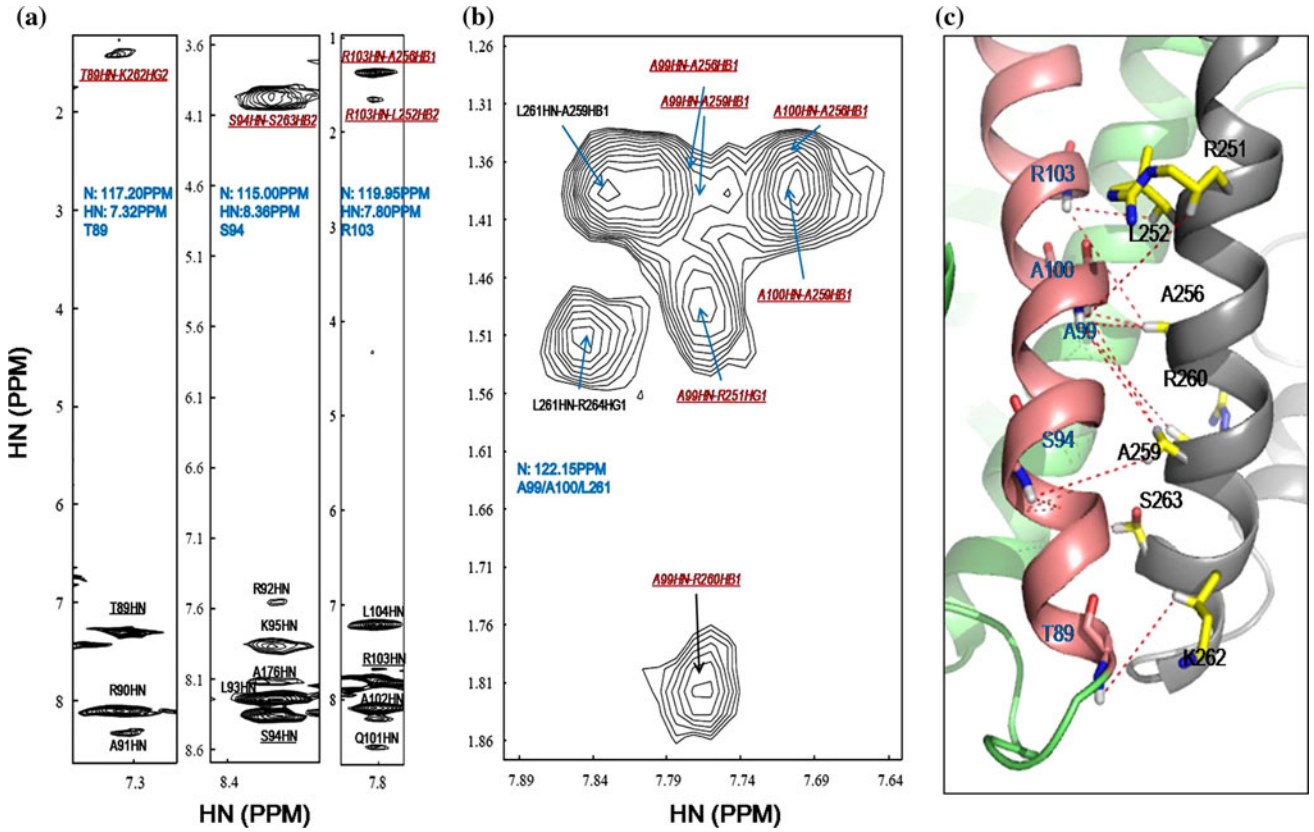

Fig. 4 Selected cross-sections of a ^{15}N-edited NOESY of this special segmental-labeled apoE3 and corresponding structure region. **a** Cross-sections of T89, S94 and R103, the diagonal peaks are *underlined*. **b** Zoom in aliphatic cross-section of A99/A100/L261. In **a** and **b**, the inter-domain NOEs are in *red* while others labeled in *black*. **c** Corresponding structure region of the residues in **a** and **b**. The residues in the CT-domain contributing to the inter-domain NOEs are displayed in *yellow sticks* and labeled in *black*, while the residues in the NT-domain only display *backbone sticks* and are labeled in *blue*. The assigned inter-domain NOEs are indicated by *red dotted lines*

^{15}N-edited and 4-D ^{15}N/^{13}C-edited NOESY spectra using 50% deuterated, uniformly triple-labeled apoE. A total of 224 inter-domain NOE distance restraints were generated finally and used for apoE3 structure determination. Figure 5 shows those inter-domain NOEs obtained mainly between a long helix (Grey) in the CT-domain and Helix 3 (Cyan) in the NT-domain (Fig. 5a), as well as between the same long helix (Grey) and Helix 4 (Cyan) in the NT-domain (Fig. 5b). Other long-range inter-domain NOEs were also observed from different regions of the CT-domain to the helices 3 and 4 of the NT-domain. These inter-domain NOEs allowed for accurate definition of the domain–domain interfaces within apoE. A striking feature was observed in Fig. 5b, showing that the positively charged Lys and Arg residues in the major low-density lipoprotein receptor (LDLR)-binding regions in Helix 4 of the NT-domain have many inter-domain NOEs with either negatively charged residues such as Asp and Glu or polar residues such as Gln and Asn in the CT-domain. This suggests that these major LDLR-binding residues in the NT-domain may form salt-bridges and H-bonds with the residues in the CT-domain through domain–domain interactions.

These results, for the first time, indicate that apoE3 contains extensive domain–domain interactions which are specific salt-bridges and H-bonds; different from the current hypothesis that apoE3 does not contain domain–domain interactions (Dong and Weisgraber 1996). However, NMR data shown in this report confirm these unambiguous domain–domain interactions in apoE3. In addition, the major LDLR-binding region is shielded by the CT-domain via domain–domain interactions, providing a possible structural reason for the inactive LDLR-binding conformation of lipid-free apoE.

The segmental labeling scheme reported here may represent a potential universal NMR approach to accurately defining the domain–domain interactions of large multi-domain proteins. Indeed, this approach allows for confident determination of the apoE3's domain–domain interactions, which is suggested to be critical to the biological functions of this important protein. This approach can be generally applied to those multi-domain proteins that contain a

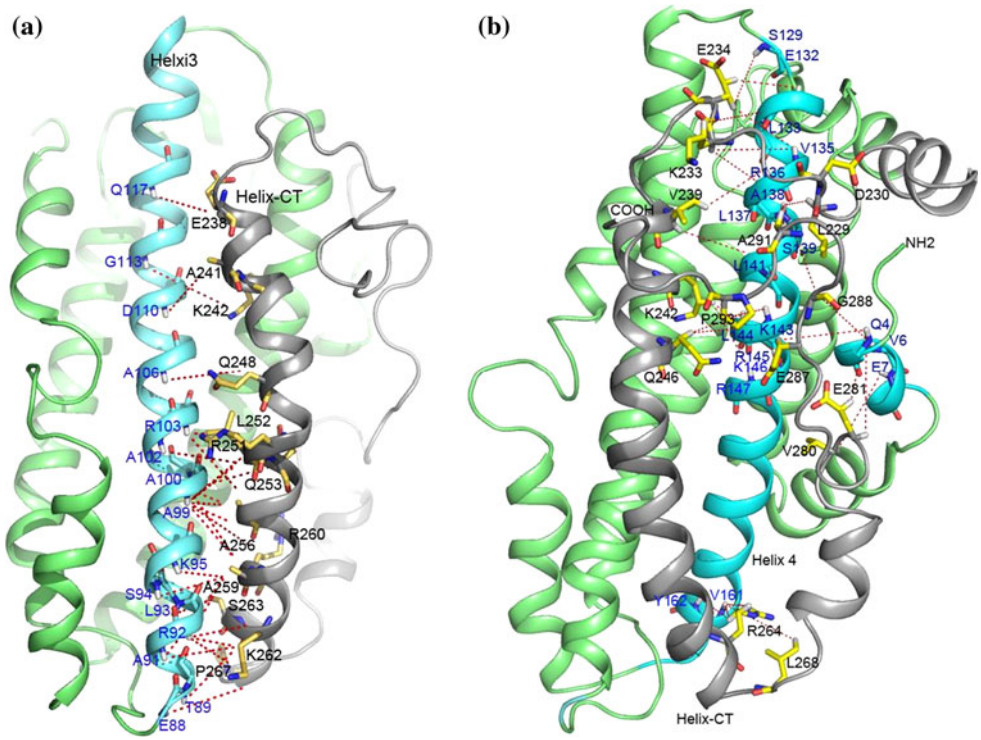

Fig. 5 Local NMR structure of apoE3 focusing on inter-domain NOEs derived from this special segmental-labeled apoE3. **a** Structural interface between apoE Helix3 in the NT-domain (*cyan*) and the long helix in the CT-domain (*gray*). **b** Structure interface between Helix4 in the NT-domain (*cyan*) and the long helix in the CT-domain (*gray*). In both **a** and **b**, the unambiguously assigned inter-domain NOEs are indicated by *red dotted lines*; the residues in the CT-domain contributing to the inter-domain NOEs are displayed in *yellow sticks*, while the residues in the NT-domain only show *backbone sticks*

relatively flexible loop between domains; the most promising application of this approach is for structure-related functional studies on apoE2 and E4 and apoE's intriguing isoform-specific effect on human diseases. Although, an efficient native ligation protocol requires expertise in molecular biology and protein chemistry, which sometime is difficult, the advantage of unambiguous observation of the inter-domain interactions of large multi-domain proteins using this special segmental labeling strategy and simple 3-D ^{15}N-edited NOESY spectra is appealing.

Acknowledgments This work is supported by NIH RO1 grant from the NIH (HL074365 to Jianjun Wang), a grant from the American Health Assistant Foundation (Jianjun Wang). The authors also thank Rebecca Wang for critical reading the manuscript.

References

Bax A (2003) Weak alignment offers new NMR opportunities to study protein structure and dynamics. Protein Sci 12(1):1–16

Burt TD, Agan BK, Marconi VC, He W, Kulkarni H, Mold JE, Cavrois M, Huang Y, Mahley RW, Dolan MJ, McCune JM, Ahuja SK (2008) Apolipoprotein (apo) e4 enhances hiv-1 cell entry in vitro, and the apoe epsilon4/epsilon4 genotype accelerates HIV disease progression. Proc Natl Acad Sci USA 105(25):8718–8723

Cui C, Zhao W, Chen J, Wang J, Li Q (2006) Elimination of in vivo cleavage between target protein and intein in the intein-mediated protein purification systems. Protein Expr Purif 50(1):74–81

Delaglio F, Grzesiek S, Vuister GW, Zhu G, Pfeifer J, Bax A (1995) NMR pipe: a multidimensional spectral processing system based on UNIX pipes. J Biomol NMR 6(3):277–293

Dong LM, Weisgraber KH (1996) Human apolipoprotein e4 domain interaction. Arginine 61 and glutamic acid 255 interact to direct the preference for very low density lipoproteins. J Biol Chem 271(32):19053–19057

Dong LM, Wilson C, Wardell MR, Simmons T, Mahley RW, Weisgraber KH, Agard DA (1994) Human apolipoprotein e. Role of arginine 61 in mediating the lipoprotein preferences of the e3 and e4 isoforms. J Biol Chem 269(35):22358–22365

Dong LM, Parkin S, Trakhanov SD, Rupp B, Simmons T, Arnold KS, Newhouse YM, Innerarity TL, Weisgraber KH (1996) Novel mechanism for defective receptor binding of apolipoprotein e2 in type iii hyperlipoproteinemia. Nat Struct Biol 3(8):718–722

Fan D, Li Q, Korando L, Jerome WG, Wang J (2004) A monomeric human apolipoprotein e carboxyl-terminal domain. Biochemistry 43(17):5055–5064

Ferrage F, Dutta K, Shekhtman A, Cowburn D (2010) Structural determination of biomolecular interfaces by nuclear magnetic resonance of proteins with reduced proton density. J Biomol NMR 47(1):41–54

Gardner KH, Kay LE (1998) The use of 2h, 13c, 15n multidimensional NMR to study the structure and dynamics of proteins. Annu Rev Biophys Biomol Struct 27:357–406

Garrett DS, Powers R, Gronenborn AM, Clore GM (1991) A common sense approach to peak picking two-, three- and four-dimensional spectra using automatic computer analysis of contour diagrams. J Magn Reson 95:214–220

Golovanov AP, Blankley RT, Avis JM, Bermel W (2007) Isotopically discriminated NMR spectroscopy: a tool for investigating complex protein interactions in vitro. J Am Chem Soc 129(20):6528–6535

Guntert P (2004) Automated NMR structure calculation with cyana. Methods Mol Biol 278:353–378

Hatters DM, Peters-Libeu CA, Weisgraber KH (2006) Apolipoprotein e structure: insights into function. Trends Biochem Sci 31(8):445–454

Huang Y (2010) Mechanisms linking apolipoprotein e isoforms with cardiovascular and neurological diseases. Curr Opin Lipidol 21(4):337–345

Huang Y, Weisgraber KH, Mucke L, Mahley RW (2004) Apolipoprotein e: diversity of cellular origins, structural and biophysical properties, and effects in Alzheimer's disease. J Mol Neurosci 23(3):189–204

Ignatova Z, Gierasch LM (2004) Monitoring protein stability and aggregation in vivo by real-time fluorescent labeling. Proc Natl Acad Sci USA 101(2):523–528

Johnson BA, Blevins RA (1994) NMR view: a computer program for the visualization and analysis of NMR data. J Biomol NMR 4:603–614

Karagiannides I, Abdou R, Tzortzopoulou A, Voshol PJ, Kypreos KE (2008) Apolipoprotein e predisposes to obesity and related metabolic dysfunctions in mice. FEBS J 275(19):4796–4809

Ma SW, Benzie IF, Yeung VT (2008) Type 2 diabetes mellitus and its renal complications in relation to apolipoprotein e gene polymorphism. Transl Res 152(3):134–142

Mahley RW, Weisgraber KH, Huang Y (2009) Apolipoprotein e: structure determines function, from atherosclerosis to alzheimer's disease to aids. J Lipid Res 50(Suppl):S183–S188

Masterson LR, Tonelli M, Markley JL, Veglia G (2008) Simultaneous detection and deconvolution of congested nmr spectra containing three isotopically labeled species. J Am Chem Soc 130(25): 7818–7819

Pervushin K, Riek R, Wider G, Wuthrich K (1997) Attenuated t2 relaxation by mutual cancellation of dipole–dipole coupling and chemical shift anisotropy indicates an avenue to NMR structures of very large biological macromolecules in solution. Proc Natl Acad Sci USA 94(23):12366–12371

Philipps B, Hennecke J, Glockshuber R (2003) Fret-based in vivo screening for protein folding and increased protein stability. J Mol Biol 327(1):239–249

Tugarinov V, Kay LE (2005) Methyl groups as probes of structure and dynamics in NMR studies of high-molecular-weight proteins. Chembiochem 6(9):1567–1577

Vitali F, Henning A, Oberstrass FC, Hargous Y, Auweter SD, Erat M, Allain FH (2006) Structure of the two most c-terminal RNA recognition motifs of ptb using segmental isotope labeling. EMBO J 25(1):150–162

Weisgraber KH (1994) Apolipoprotein e: structure-function relationships. Adv Protein Chem 45:249–302

Weisgraber KH, Rall SC Jr, Mahley RW (1981) Human e apoprotein heterogeneity. Cysteine-arginine interchanges in the amino acid sequence of the apo-e isoforms. J Biol Chem 256(17):9077–9083

Wilson C, Mau T, Weisgraber KH, Wardell MR, Mahley RW, Agard DA (1994) Salt bridge relay triggers defective LDL receptor binding by a mutant apolipoprotein. Structure 2(8):713–718

Zhang Y, Vasudevan S, Sojitrawala R, Zhao W, Cui C, Xu C, Fan D, Newhouse Y, Balestra R, Jerome WG, Weisgraber K, Li Q, Wang J (2007) A monomeric, biologically active, full-length human apolipoprotein e. Biochemistry 46(37):10722–10732

Zhang Y, Chen J, Wang J (2008) A complete backbone spectral assignment of lipid-free human apolipoprotein e (apoe). Biomol NMR Assign 2(2):207–210

Zhao W, Zhang Y, Cui C, Li Q, Wang J (2008) An efficient on-column expressed protein ligation strategy: application to segmental triple labeling of human apolipoprotein e3. Protein Sci 17(4):736–747